Acta Cryst. (1998). B**54**, 277–290

Structural, Thermodynamic and Kinetic (Hysteresis) Aspects of the Enantiotropic First-Order Phase Transformations of *N*-Anilinophthalimide and *N*-(*N*′-Methylanilino)phthalimide

MARK BOTOSHANSKY,[a] ARKADY ELLERN,[b] NOGA GASPER,[a] JAN-OLAV HENCK[b] AND FRANK H. HERBSTEIN[a]*

[a]*Department of Chemistry, Technion-Israel Institute of Technology, Haifa 32000, Israel, and* [b]*Department of Chemistry, Ben Gurion University of the Negev, Beer Sheba 84105, Israel. E-mail: chr03fh@tx.technion.ac.il*

(*Received 24 March 1997; accepted 15 September 1997*)

Abstract

The crystal structures of the orthorhombic and monoclinic polymorphs of *N*-anilinophthalimide (m.p. of monoclinic polymorph 457 K) have been determined by X-ray diffraction at 293 K and were found to have only small differences between the molecular conformations in the two phases, but quite different molecular arrangements. There is very weak N—H···O hydrogen bonding in the orthorhombic phase and weak N—H···O hydrogen bonding in the monoclinic phase. The thermal motion in the crystals of both phases has been analyzed and their thermal expansion determined. The enthalpies of solution in a number of solvents have been calculated from the solubility measurements of Chattaway & Lambert [(1915), *J. Chem. Soc.* **107**, 1773–1781], which also give the temperature and enthalpy of the enantiotropic 'orthorhombic to monoclinic' phase transformation (T_c = 283 K; ΔH_{transf} = 1.54 kJ mol^{-1}). The phase-transformation endotherm in a DSC (differential scanning calorimetry) trace from the orthorhombic polymorph occurs only at ~310 K on heating and there is no corresponding exotherm on cooling; the DSC trace gives ΔH_{transf} = 1.62 kJ mol^{-1} and ΔH_{fus} = 26.9 kJ mol^{-1}. This phase transformation is an example of the common type (occurrence ~95%) where ΔV_{transf} = ($V_{monoclinic}$ − $V_{orthorhombic}$) is positive. Analogous (but less complete) results have been obtained for the monoclinic and triclinic polymorphs of *N*-(*N*′-methylanilino)phthalimide (m.p. of triclinic polymorph 398 K). There were only minor differences between the molecular conformations in the two phases, but the molecular arrangements were quite different. This 'monoclinic to triclinic' phase transformation also has ΔV_{transf} = ($V_{triclinic}$ − $V_{monoclinic}$) positive. The solubility (and other) measurements of Chattaway & Lambert (1915) gave T_c = 328.43 K and ΔH_{transf} = 4.17 kJ mol^{-1}. A DSC trace for the monoclinic crystals shows a broad endotherm at ~372–376 K on heating, but there is no corresponding exotherm on cooling; ΔH_{transf} = 3.6 kJ mol^{-1} and ΔH_{fus} = 21.7 kJ mol^{-1}. These two compounds provide further examples of molecular crystals with a large hysteresis in their first-order enantiotropic solid-state phase transformations, the transformation to the high-temperature phase occurring well above T_c and the low-temperature phase not being recovered on cooling below T_c. Presumably the hysteresis must be ascribed to as-yet unknown features of the nucleation processes.

1. Introduction

Polymorphism† frequently occurs in organic crystals (Gavezzotti & Filippini, 1995; GF95) and its investigation requires an integration of structural and thermodynamic studies (Herbstein, 1996). However, it is not often that both types of information are available, or easily obtainable, for the same system. The preferred source of thermodynamic information is the heat capacity at constant pressure (usually 1 atm.) as a function of temperature; unfortunately, such measurements are comparatively rare. It would always be desirable to have pressure as an additional variable, but this is even less available. Alternatively, solubility measurements (as a function of temperature) for both polymorphs can give direct experimental information about the temperature and enthalpy of transformation, from which the entropy of transformation can be calculated. Thus, the availability of such measurements for 'phthalylphenylhydrazide' (now called *N*-anilinophthalimide‡) and 'phthalylphenylmethylhydrazide' [now called *N*-(*N*′-methylanilino)phthalimide (Chattaway & Wünsch, 1911 (CW11); Chattaway & Lambert, 1915 (CL15)] provided an incentive to determine the crystal structures of these pairs of polymorphs ('clusters' in the nomenclature of GF95) in order to study the relationship between their structures and thermodynamic properties. Both compounds show first-order enantiotropic§ transitions between the two phases *A* and *B*. The solubility–temperature curves of the two polymorphs have similar (but not identical) slopes and curvatures (Figs. 1 and 2 of CL15). The crystallography of the two pairs of polymorphs was established by T. V.

† Defined briefly as 'the appearance of differenct crystal structures for the same molecule', following Gavezzotti & Filippini (1995).

‡ The occurrence of two 'physical isomers' of this compound was investigated by Dunlap (1905), who also reviewed earlier work.

§ For (standard) definitions of 'order of a transition' and 'enantiotropic' see Herbstein (1996).

Barker using (optical) goniometric methods (these results were not published separately but included in CW11); analogous results for *N*-anilinophthalimide had earlier been obtained by E. H. Kraus and quoted by Dunlap (1905). We now report the crystal structures of the orthorhombic and monoclinic polymorphs of *N*-anilinophthalimide, and of the monoclinic and triclinic polymorphs of *N*-(*N*′-methylanilino)phthalimide. The crystal structure of the triclinic polymorph of *N*-(*N*′-methylanilino)phthalimide has been reported (Barlow *et al.*, 1979), although the authors do not appear to have been aware of the earlier work of Chattaway and colleagues.

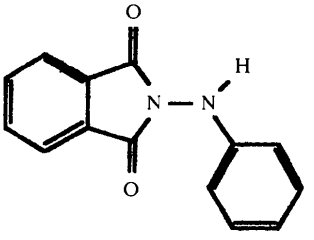

N-Anilinophthalimide

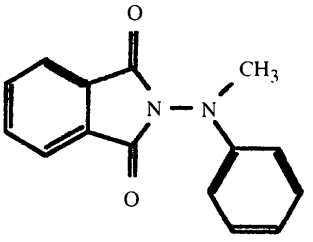

N-(*N*′-Methylanilino)phthalimide

(1)

The *N*-anilinophthalimide and *N*-(*N*′-methylanilino)phthalimide systems provide an added kinetic dividend because their phase transformations are characterized by marked hysteresis. It is well known that there are many systems in which phase *A* can be superheated above T_c and phase *B* supercooled below T_c. A partial list, given by Rao & Gopalakrishnan (1989), includes CsCl, AgI, NH_4Cl and $RbBO_3$, to which can be added SiO_2 as cristabolite and quartz. These examples can perhaps be explained by invoking the need to break and re-form covalent bonds in the case of SiO_2, or transform strongly bound ionic arrangements in the other examples. However, similar situations do occur in crystals with weaker interactions between the structural units. An example with a long history is thallium(I) picrate, first described in 1866 as crystallizing as yellow needles and, 2 years later, also as red prisms. More extended investigation (Rabe, 1901; Cohen & Moesveld, 1920) showed that, at about neutral pH, yellow needles of Tl^I picrate crystallize first, irrespective of crystallization temperature. The yellow needles change over a few days to red prisms if left in contact with solvent at room temperature, but both needles and prisms are indefinitely stable at room temperature under dry conditions. Rabe (1901) investigated the relative stabilities of the two phases by measuring their solubilities in water and methanol as a function of temperature (see *Appendix*); his conclusion was: 'Das Thallopikrat tritt in zwei physikalisch isomeren Formen auf, deren Umwandlungspunkt bei 46°C liegt'. He also reported that there was instantaneous transformation of red to yellow at 403 K and above. The transformation was found to be remarkably accelerated by the presence of small amounts of solvent. Cohen & Moesveld (1920) [see also Cohen (1929)] confirmed the transition point as 319 K from dilatometric measurements (they used 150 g of each of the red and yellow polymorphs and moistened their samples to accelerate the transformation) and found ΔV to be ~6%. We have reported the crystal structures of the red (Herbstein *et al.*, 1977) and yellow phases (Botoshansky *et al.*, 1994*a*), which are both monoclinic, and studied the relationship and transformations between them. Similar phenomena were reported in the *N*-anilinophthalimide and *N*-(*N*′-methylanilino)phthalimide systems (CW11, CL15). For example, it was noted (see p. 1778 of CL15) that the solubility of *N*-anilinophthalimide in ethanol is 'so small, and the rate of transformation at the ordinary temperature so slow, that crystals of the two modifications suspended in a saturated alcoholic solution remain for months without any apparent alteration...Similar tubes containing the yellow form seeded with the pale form and kept at 0°C in an ice-box for a month showed no apparent change'. Pyridinium picrate could well be another example of similar behavior (Botoshansky *et al.*, 1994*b*).

2. Crystal structure analyses

2.1. *Preparation of crystals of the polymorphs of N-anilinophthalimide*

The literature instructions for synthesis of *N*-anilinophthalimide (condensation of phthalic anhydride and phenylhydrazine in dioxane, followed by elimination of water by heating at 373 K) were not successful unless a small amount of toluenesulfonic acid was added to the reaction mixture (see Becker *et al.*, 1998). The α- and β-forms were obtained by slow cooling following the recipes of CW11; Dunlap (1905) gives similar prescriptions.

2.2. *Comparison with earlier results for N-anilinophthalimide*

Barker determined the axial ratios of the α-polymorph as $a:b:c$ = 1.0875:1:0.5568. Our values are

1.8409:1:0.5154. If Barker's a and b are interchanged and the new a is doubled we obtain 1.8391:1:0.5120; Kraus (quoted by Dunlap, 1905) gave 0.2526:1:0.9118, easily convertible to our values. Barker gave for the β-polymorph $a:b:c$ = 1.1573:1:1.204 and β = 126.26°. Multiplication of the Barker axial set by ($\bar{1}00$, $0\bar{1}0$, 101) gives our cell. Kraus gave 1.1671:1:0.7848 and β = 54.8°, again convertible to our cell. Thus, there is good agreement between the Barker and Kraus goniometric and our diffraction results. We find ΔV_{transf} ($=V_{monoclinic} - V_{orthorhombic}$) = 5.5 Å^3 per molecule or 1.9%, considerably larger than the value of −0.5% derived from the measured densities cited in CW11; our remeasurement of the crystal densities resolves the discrepancy. This pair of polymorphs shows the situation most common (frequency ~95%) in an enantiotropic system, the higher-temperature modification being the less dense.

2.3. *Preparation of crystals of the polymorphs of N-(N′-methylanilino)phthalimide*

Crystals of the triclinic polymorph were obtained by condensation of phthalic anhydride and methylphenylhydrazine in dioxane, followed by elimination of water by heating at 373 K. The triclinic polymorph did not transform (in our hands) at room temperature in the presence of solvent to the monoclinic polymorph, as stated by CL15 (p. 1778). For some time we suspected that we had encountered another example of a disappearing polymorph (Dunitz & Bernstein, 1995; see also *Acknowledgements*), but eventually stirring for 8 h of an orange-colored suspension of the triclinic polymorph in 96% ethanol at 318 K (just below T_c) showed a transformation to yellow. Slow cooling to room temperature (without stirring) gave crystals of the (pale yellow) monoclinic polymorph after 24 h.

2.4. *Comparison with earlier results for N-(N′-methylanilino)phthalimide*

Barker measured the axial ratios of the monoclinic polymorph as $a:b:c$ = 0.7659:1:0.5306, β = 92.17°; density (21/4°; method not specified) = 1.327 Mg m^{-3}, molar volume 189.9. We find $a:b:c$ = 0.5322:1:0.7632, β = 92.25° (Table 1); thus, we and the Chattaway group are dealing with the same crystals. Our density measurement (flotation in aqueous KI) gave 1.327 Mg m^{-3}.

Barker gave for the triclinic polymorph $a:b:c$ = 0.5853:1:0.3801 and α = 110.0, β = 114.23, γ = 68.28°; density (16/4°) = 1.352 Mg m^{-3}, molar volume 186.5 cm^3. Using BLAF (Macicek & Yordanov, 1992) these values can be converted into a 'dummy' reduced cell with a = 5.704, b = 8.276, c = 14.114 Å, α = 74.38, β = 87.68, γ = 75.35°. The cell given by Barlow *et al.* (1979) can be reduced to give a = 5.704, b = 8.370, c = 14.210 Å, α = 74.42, β = 87.76, γ = 75.20°, density = 1.32 Mg m^{-3}. Matrix multiplication of the original Barker and Barlow axial sets by (001, 101, 011) and (001, 100, 110), respectively, gives the reduced cell. Clearly Barker and Barlow studied the same crystals and we have confirmed their results in our repetition of the Barlow crystal structure analysis. Our density measurement (flotation in aqueous KI) gave 1.295 Mg m^{-3}.

We calculate ΔV_{transf} ($= V_{triclinic} - V_{monoclinic}$) = 3.9 Å^3 per molecule or 1.25%. The calculations of ΔV_{transf} are based on the diffraction measurements of cell volumes, which are more reliable than densities.

3. Structure determinations

As similar techniques were used for all four crystals investigated here, much of the description is common and only differences will be emphasized. After preliminary surveys of crystal quality and parameters by oscillation and Weissenberg photography, cell-dimension and intensity measurements were made on a four-circle diffractometer, using graphite-monochromated Mo $K\alpha$ radiation (Table 1). We consider the results mostly on a pairwise basis (*e.g.* crystal structures), but for some aspects (*e.g.* molecular geometry) the comparison extends over all four molecules.

Atomic parameters for the two polymorphs of *N*-anilinophthalimide are in Tables 2 and 3. Atomic parameters for the polymorphs of *N*-(*N*′-methylanilino)phthalimide are in Tables 4 and 5.† The numbering of the atoms is shown in Fig. 1.

4. Geometry of *N*-anilinophthalimide and *N*-(*N*′-methylanilino)phthalimide molecules

Bond lengths for the four polymorphs are given in Table 6; bond angles have been deposited, but some selected bond and torsion angles are in Table 7. There is an overall resemblance among the conformations of both molecules in the four polymorphs in the sense that the planes of the phenyl and phthalimide rings are approximately mutually perpendicular, although torsion angles around the N—C(phenyl) bonds differ somewhat in detail. In particular, the conformations of the two independent molecules of the monoclinic polymorph of *N*-anilinophthalimide differ little, but are significantly different from that found in the orthorhombic polymorph. The conformations of the molecules in the monoclinic and triclinic polymorphs of *N*-(*N*′-methylanilino)phthalimide also show small but significant differences. These differences can be

† Lists of hydrogen coordinates, anisotropic displacement parameters and structure factors, and details of molecular geometries for all four phases have been deposited with the IUCr (Reference: BK0046). Copies may be obtained through The Managing Editor, International Union of Crystallography, 5 Abbey Square, Chester CH1 2HU, England.

Table 1. *Experimental details*

	(1)	(2)	(3)	(4)
Crystal data				
Chemical formula	$C_{14}H_{10}N_2O_2$	$C_{14}H_{10}N_2O_2$	$C_{15}H_{12}N_2O_2$	$C_{15}H_{12}N_2O_2$
Chemical formula weight	238.24	238.24	252.27	252.27
Cell setting	Orthorhombic	Monoclinic	Monoclinic	Triclinic
Space group	$P2_12_12_1$	$P2_1/a$	$P2_1/c$	$P\bar{1}$
a (Å)	19.655 (6)	14.724 (4)	7.752 (3)	5.745 (2)
b (Å)	10.677 (3)	12.664 (3)	14.567 (4)	8.347 (3)
c (Å)	5.503 (2)	13.970 (3)	11.118 (3)	14.213 (4)
α (°)				74.45
β (°)		115.38 (3)	92.25 (2)	87.75
γ (°)				75.39
V (Å^3)	1154.8 (6)	2353.5 (10)	1254.5 (7)	635.1 (4)
Z	4	8	4	2
D_x (Mg m^{-3})	1.370	1.345	1.338	1.319
D_m (Mg m^{-3})	1.377	1.341	1.327	1.295
Density measured by	Flotation	Flotation	Flotation	Flotation
Radiation type	Mo $K\alpha$	Mo $K\alpha$	Mo $K\alpha$	Mo $K\alpha$
Wavelength (Å)	0.71070	0.71070	0.71073	0.71073
No. of reflections for cell parameters	25	25	40	40
θ range (°)	2.4–12.6	2.1–8.5	15–18	15–18
μ (mm^{-1})	0.094	0.092	0.091	0.090
Temperature (K)	293 (2)	293 (2)	293 (2)	293 (2)
Crystal form	Plate	Plate	Transparent prism with well shaped faces	Prism
Crystal size (mm)	1.13 × 0.28 × 0.07	0.5 × 0.3 × 0.1	0.40 × 0.30 × 0.27	0.4 × 0.4 × 0.2
Crystal color	Light yellow	Deep yellow	Pale yellow	Orange
Data collection				
Diffractometer	Philips PW 1100 four-circle	Philips PW 1100 four-circle</entry	Syntex P$\bar{1}$	Syntex P$\bar{1}$
Data collection method	$\omega/2\theta$ scans	$\omega/2\theta$ scans	$\omega/2\theta$ scans	$\omega/2\theta$ scans
Absorption correction	None	None	None	None
No. of measured reflections	1224	4327	2663	2253
No. of independent reflections</entry	1224	4150	2480	2018
No. of observed reflections	835	2842	1620	1340
Criterion for observed reflections	$I > 2\sigma(I)$	$I > 2\sigma(I)$	$I > 2\sigma(I)$	$I > 2\sigma(I)$
R_{int}	–	0.0395	0.0098	0.0144
θ_{max} (°)	25.00	24.99	26.06	24.05
Range of h, k, l	$0 \rightarrow h \rightarrow 23$ $0 \rightarrow k \rightarrow 12$ $0 \rightarrow l \rightarrow 6$	$-17 \rightarrow h \rightarrow 15$ $0 \rightarrow k \rightarrow 15$ $0 \rightarrow l \rightarrow 16$	$0 \rightarrow h \rightarrow 9$ $0 \rightarrow k \rightarrow 18$ $-13 \rightarrow l \rightarrow 13$	$0 \rightarrow h \rightarrow 6$ $-9 \rightarrow k \rightarrow 9$ $-16 \rightarrow l \rightarrow 16$
No. of standard reflections</entry	3	3	2	2
Frequency of standard reflections	120 min	120 min	Every 98 reflections	Every 98 reflections
Intensity decay (%)	2.0	2.4	0.8	None
Refinement				
Refinement on	F^2	F^2	F^2	F^2
$R[F^2 > 2\sigma(F^2)]$	0.0555	0.0640	0.0450	0.0403
$wR(F^2)$	0.1200	0.1968	0.1495	0.1175
S	1.203	1.159	1.216	1.248
No. of reflections used in refinement	1224	4150	2472	2018
No. of parameters used	204	406	173	221
H-atom treatment	All H-atom parameters refined	All H-atom parameters refined	All H-atom parameters refined	All H-atom parameters refined
Weighting scheme	$w = 1/[\sigma^2(F_o^2) + (0.0269P)^2 + 0.2144P]$, where $P = (F_o^2 + 2F_c^2)/3$	$w = 1/[\sigma^2(F_o^2) + (0.1021P)^2 + 0.5912P]$, where $P = (F_o^2 + 2F_c^2)/3$	$w = 1/[\sigma^2(F_o^2) + (0.1000P)^2 + 0.0000P]$, where $P = (F_o^2 + 2F_c^2)/3$	$w = 1/[\sigma^2(F_o^2) + (0.0800P)^2 + 0.0000P]$, where $P = (F_o^2 + 2F_c^2)/3$
$(\Delta/\sigma)_{max}$	0.030	0.012	0.001	−0.007

Table 1 (*cont.*)

	(1)	(2)	(3)	(4)
$\Delta\rho_{max}$(e Å^{-3})	0.17	0.22	0.21	0.17
$\Delta\rho_{min}$ (e Å^{-3})	−0.15	−0.18	−0.16	−0.13
Extinction method	*SHELXL*93 (Sheldrick, 1993)	*SHELXL*93 (Sheldrick, 1993)	*SHELXL*93 (Sheldrick, 1993)	*SHELXL*93 (Sheldrick, 1993)
Extinction coefficient	0.0226 (44)	0.0002 (10)	0.0358 (68)	0.0363 (82)
Source of atomic scattering factors	*International Tables for Crystallography* (Vol. C)	*International Tables for Crystallography* (Vol. C)	*International Tables for Crystallography* (Vol. C)	*International Tables for Crystallography* (Vol. C)
Computer programs				
Data collection	*PW* 1100/20 (Philips, 1973)	*PW* 1100/20 (Philips, 1973)	*P3/PC* (Siemens, 1989*a*)	*P3/PC* (Siemens, 1989*a*)
Cell refinement	*PW* 1100/20 (Philips, 1973)	*PW* 1100/20 (Philips, 1973)	*P3/PC* (Siemens, 1989*a*)	*P3/PC* (Siemens, 1989*a*)
Data reduction	*PW* 1100/20 (Philips, 1973)	*PW* 1100/20 (Philips, 1973)	*XDISK* (Siemens, 1989*b*)	*XDISK* (Siemens, 1989*b*)
Structure solution	*SHELXS*86 (Sheldrick, 1990)	*SHELXS*86 (Sheldrick, 1990)	*SHELXS*86 (Sheldrick, 1990)	*SHELXS*86 (Sheldrick, 1990)
Structure refinement	*SHELXL*93 (Sheldrick, 1993)	*SHELXL*93 (Sheldrick, 1993)	*SHELXL*93 (Sheldrick, 1993)	*SHELXL*93 (Sheldrick, 1993)
Preparation of material for publication	MS Word 6.0.1 for Macintosh	MS Word 6.0.1 on Macintosh	MS Word 6.0.1 for Macintosh	MS Word 6.0.1 for Macintosh

ascribed to 'packing effects' and involve relatively small energies. However, there are also some differences (~0.02 Å) in bond lengths which are formally significant, but difficult to explain; underestimation of standard uncertainties (Taylor & Kennard, 1986) must play some role. The disposition of bonds about the phthalimide nitrogen N1 (mean angles ≃ 123, 123 and 113°) is essentially planar in all four polymorphs, while N2 is pyramidal (mean angles are ≃ 114, 114 and 119°; Table 7).

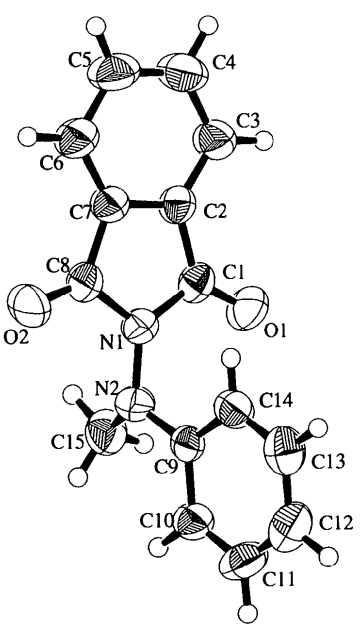

Fig. 1. *ORTEP*II diagram (Johnson, 1976) of the *N*-(*N*′-methylanilino)phthalimide molecule in the monoclinic phase, showing the numbering of atoms and thermal ellipsoids at 50% probability levels. H atoms have been given arbitrary, but convenient, radii. The corresponding diagram for the molecule in the triclinic phase is rather similar, as are those for the two phases of *N*-anilinophthalimide, where the methyl group is replaced by HN_2.

5. Crystal structures of *N*-anilinophthalimide and *N*-(*N*′-methylanilino)phthalimide

5.1. *Molecular packing of N-anilinophthalimide*

The packing arrangements in the two polymorphs are illustrated in the stereo diagrams of Figs. 2 and 3. We have not been able to detect any resemblances between the two packing arrangements, nor to find really adequate descriptions. There is a very weak hydrogen bond from O2 to HN2 (of the molecule at $x, y, -1 + z$) in the orthorhombic polymorph [Table 8; d(N···O) = 3.407 (6) Å]. There is a weak O···H—C interaction [d(O···H) = 2.37 Å] between O1 of the reference

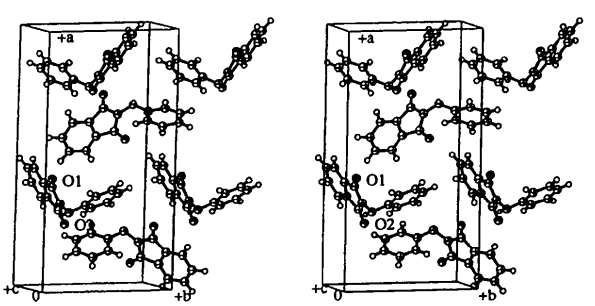

Fig. 2. *ORTEP*II (Johnson, 1976) stereodiagram showing the packing in the orthorhombic polymorph of *N*-anilinophthalimide; viewed approximately down [001]. Details as for Fig. 1.

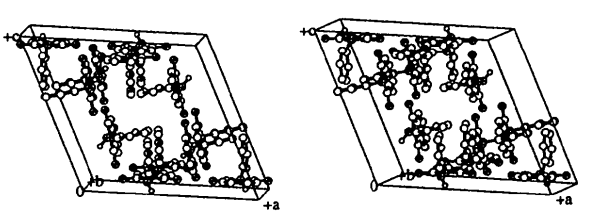

Fig. 3. *ORTEP*II (Johnson, 1976) stereodiagram showing the packing in the monoclinic polymorph of *N*-anilinophthalimide; viewed approximately down [100]. Details as for Fig. 1.

Table 2. *Fractional atomic coordinates and equivalent isotropic displacement parameters (Å²) for the α-polymorph (orthorhombic) of N-anilinophthalimide*

$U_{eq} = (1/3)\Sigma_i\Sigma_j U^{ij} a^i a^j \mathbf{a}_i.\mathbf{a}_j$.

	x	y	z	U_{eq}
C1	0.3958 (2)	0.0909 (5)	0.1822 (10)	0.0632 (14)
C2	0.4179 (2)	−0.0103 (4)	0.0176 (8)	0.0525 (12)
C3	0.4746 (3)	−0.0862 (6)	0.0259 (12)	0.069 (2)
C4	0.4812 (3)	−0.1763 (5)	−0.1568 (12)	0.068 (2)
C5	0.4327 (2)	−0.1893 (5)	−0.3379 (10)	0.0650 (15)
C6	0.3757 (2)	−0.1126 (5)	−0.3440 (10)	0.0587 (13)
C7	0.3687 (2)	−0.0227 (4)	−0.1666 (9)	0.0503 (11)
C8	0.3154 (2)	0.0730 (4)	−0.1289 (8)	0.0546 (12)
C9	0.3223 (2)	0.3504 (4)	0.1849 (8)	0.0500 (11)
C10	0.3057 (3)	0.4381 (6)	0.3652 (9)	0.0628 (14)
C11	0.3277 (3)	0.5604 (5)	0.3461 (10)	0.0631 (14)
C12	0.3683 (3)	0.5985 (5)	0.1582 (11)	0.0645 (14)
C13	0.3859 (3)	0.5115 (5)	−0.0208 (10)	0.0648 (15)
C14	0.3632 (3)	0.3903 (5)	−0.0077 (9)	0.0573 (13)
N1	0.3337 (2)	0.1349 (4)	0.0888 (7)	0.0536 (10)
N2	0.2946 (2)	0.2295 (4)	0.1945 (9)	0.0599 (12)
O1	0.4216 (2)	0.1334 (3)	0.3672 (7)	0.0812 (12)
O2	0.2657 (2)	0.0970 (3)	−0.2519 (6)	0.0651 (10)

Table 3. *Fractional atomic coordinates and equivalent isotropic displacement parameters (Å²) for the β-polymorph (monoclinic) of N-anilinophthalimide*

$U_{eq} = (1/3)\Sigma_i\Sigma_j U^{ij} a^i a^j \mathbf{a}_i.\mathbf{a}_j$.

	x	y	z	U_{eq}
C1*A*	0.4891 (2)	0.1538 (2)	0.0989 (2)	0.0516 (7)
C2*A*	0.4637 (2)	0.2658 (2)	0.0995 (2)	0.0477 (6)
C3*A*	0.5170 (2)	0.3561 (2)	0.1031 (3)	0.0614 (8)
C4*A*	0.4718 (3)	0.4521 (3)	0.1037 (3)	0.0673 (8)
C5*A*	0.3757 (3)	0.4566 (3)	0.0998 (3)	0.0638 (8)
C6*A*	0.3227 (2)	0.3672 (2)	0.0969 (2)	0.0537 (7)
C7*A*	0.3670 (2)	0.2719 (2)	0.0955 (2)	0.0469 (6)
C8*A*	0.3284 (2)	0.1634 (2)	0.0901 (2)	0.0496 (6)
C9*A*	0.4390 (2)	−0.0781 (2)	0.1696 (2)	0.0519 (7)
C10*A*	0.4412 (2)	−0.1859 (2)	0.1510 (3)	0.0621 (8)
C11*A*	0.4745 (3)	−0.2542 (3)	0.2364 (4)	0.0787 (10)
C12*A*	0.5040 (3)	−0.2191 (3)	0.3380 (3)	0.0792 (10)
C13*A*	0.5033 (3)	−0.1124 (3)	0.3557 (3)	0.0759 (10)
C14*A*	0.4709 (2)	−0.0420 (3)	0.2717 (3)	0.0646 (8)
N1*A*	0.4080 (2)	0.0970 (2)	0.0969 (2)	0.0513 (6)
N2*A*	0.3964 (2)	−0.0108 (2)	0.0806 (2)	0.0611 (7)
O1*A*	0.56548 (15)	0.1137 (2)	0.0998 (2)	0.0689 (6)
O2*A*	0.24743 (15)	0.1332 (2)	0.0819 (2)	0.0687 (6)
C1*B*	0.2838 (2)	0.1482 (2)	−0.2226 (2)	0.0535 (7)
C2*B*	0.2746 (2)	0.2609 (2)	−0.2541 (2)	0.0527 (7)
C3*B*	0.2828 (2)	0.3503 (3)	−0.1953 (3)	0.0606 (8)
C4*B*	0.2732 (3)	0.4471 (3)	−0.2445 (3)	0.0727 (9)
C5*B*	0.2562 (3)	0.4524 (3)	−0.3499 (3)	0.0795 (10)
C6*B*	0.2473 (3)	0.3636 (3)	−0.4088 (3)	0.0701 (9)
C7*B*	0.2561 (2)	0.2673 (2)	−0.3595 (2)	0.0562 (7)
C8*B*	0.2513 (2)	0.1584 (3)	−0.4015 (2)	0.0611 (8)
C9*B*	0.1916 (2)	−0.0796 (2)	−0.3377 (2)	0.0596 (7)
C10*B*	0.2036 (3)	−0.1876 (3)	−0.3343 (3)	0.0731 (9)
C11*B*	0.1218 (4)	−0.2528 (3)	−0.3552 (3)	0.0876 (12)
C12*B*	0.0284 (4)	−0.2111 (4)	−0.3800 (3)	0.0934 (13)
C13*B*	0.0162 (3)	−0.1039 (4)	−0.3851 (3)	0.0855 (11)
C14*B*	0.0972 (2)	−0.0375 (3)	−0.3648 (3)	0.0704 (9)
N1*B*	0.2680 (2)	0.0924 (2)	−0.3147 (2)	0.0620 (7)
N2*B*	0.2779 (2)	−0.0166 (2)	−0.3195 (3)	0.0732 (8)
O1*B*	0.3018 (2)	0.1085 (2)	−0.1377 (2)	0.0752 (7)
O2*B*	0.2367 (2)	0.1289 (2)	−0.4888 (2)	0.0848 (8)

Table 4. *Fractional atomic coordinates and equivalent isotropic displacement parameters (Å²) for the α-polymorph (monoclinic) of N-(N′-methylanilino)phthalimide*

$U_{eq} = (1/3)\Sigma_i\Sigma_j U^{ij} a^i a^j \mathbf{a}_i.\mathbf{a}_j$.

	x	y	z	U_{eq}
C1	0.7301 (2)	0.02520 (11)	0.16114 (14)	0.0481 (4)
C2	0.7582 (2)	0.02885 (11)	0.03043 (14)	0.0472 (4)
C3	0.7174 (2)	−0.03368 (12)	−0.0589 (2)	0.0570 (5)
C4	0.7549 (3)	−0.00993 (14)	−0.1758 (2)	0.0639 (5)
C5	0.8309 (2)	0.07322 (14)	−0.20057 (14)	0.0604 (5)
C6	0.8725 (2)	0.13618 (12)	−0.11090 (15)	0.0540 (4)
C7	0.8350 (2)	0.11277 (10)	0.00492 (14)	0.0447 (4)
C8	0.8617 (2)	0.16495 (11)	0.11860 (14)	0.0461 (4)
C9	0.6202 (2)	0.15567 (10)	0.36807 (14)	0.0458 (4)
C10	0.5669 (3)	0.12686 (14)	0.47855 (15)	0.0600 (5)
C11	0.4074 (3)	0.15413 (15)	0.5185 (2)	0.0693 (6)
C12	0.3023 (3)	0.20944 (15)	0.4493 (2)	0.0705 (6)
C13	0.3536 (3)	0.23721 (14)	0.3382 (2)	0.0728 (6)
C14	0.5130 (2)	0.21097 (12)	0.2975 (2)	0.0581 (5)
C15	0.9032 (3)	0.07874 (15)	0.4055 (2)	0.0639 (5)
O2	0.9268 (2)	0.23910 (8)	0.13605 (10)	0.0644 (4)
O1	0.6672 (2)	−0.03385 (9)	0.22120 (11)	0.0687 (4)
N1	0.7918 (2)	0.10943 (9)	0.20695 (11)	0.0470 (4)
N2	0.7879 (2)	0.13429 (10)	0.32813 (11)	0.0493 (4)

Table 5. *Fractional atomic coordinates and equivalent isotropic displacement parameters (Å²) for the β-polymorph (triclinic) of N-(N′-methylanilino)phthalimide*

$U_{eq} = (1/3)\Sigma_i\Sigma_j U^{ij} a^i a^j \mathbf{a}_i.\mathbf{a}_j$.

	x	y	z	U_{eq}
C1	0.5077 (3)	1.1137 (2)	0.72181 (13)	0.0512 (5)
C2	0.4689 (3)	1.1872 (2)	0.80624 (13)	0.0499 (5)
C3	0.5631 (4)	1.3098 (3)	0.8277 (2)	0.0660 (6)
C4	0.4889 (5)	1.3578 (3)	0.9118 (2)	0.0794 (7)
C5	0.3234 (5)	1.2873 (3)	0.9712 (2)	0.0804 (7)
C6	0.2304 (4)	1.1635 (3)	0.9503 (2)	0.0699 (6)
C7	0.3069 (3)	1.1142 (2)	0.86691 (13)	0.0528 (5)
C8	0.2445 (3)	0.9846 (3)	0.82574 (13)	0.0564 (5)
C9	0.5652 (3)	0.7636 (2)	0.67052 (11)	0.0456 (5)
C10	0.5725 (4)	0.6750 (3)	0.59929 (14)	0.0577 (5)
C11	0.7735 (5)	0.5500 (3)	0.5916 (2)	0.0716 (6)
C12	0.9741 (5)	0.5097 (3)	0.6516 (2)	0.0740 (7)
C13	0.9669 (4)	0.5961 (3)	0.7218 (2)	0.0664 (6)
C14	0.7662 (3)	0.7209 (2)	0.73216 (14)	0.0549 (5)
C15	0.1871 (4)	0.9760 (3)	0.5970 (2)	0.0658 (6)
O1	0.6225 (3)	1.1472 (2)	0.64991 (10)	0.0670 (4)
O2	0.1124 (3)	0.8920 (2)	0.85656 (11)	0.0841 (5)
N1	0.3751 (3)	0.9882 (2)	0.74095 (10)	0.0527 (4)
N2	0.3571 (3)	0.8885 (2)	0.67932 (10)	0.0545 (4)

molecule and H4 of the molecule at $(1 - x, \frac{1}{2} + y, \frac{1}{2} - z)$. In the monoclinic polymorph there is weak bifurcated hydrogen bonding from O1*A* to H2N*A* and H2N*B* of the *A* and *B* molecules at $1 - x$, $-y$, $-z$ [Table 8; d(N···O) = 3.095 (3) and 3.191 (3) Å] and also from O1*B* to H2N*A* of the reference molecules [Table 8; d(N···O) = 3.144 (3) Å]. Another possible interaction is between a carbonyl group of one reference molecule to the phthalimide nitrogen of the other

Table 6. *Comparison of bond lengths in the molecules of N-anilinophthalimide and N-(N′-methylanilino)phthalimide*

Atom pair	Orthorhombic	Monoclinic *A*	Monoclinic *B*	*N*-(*N*′-Methylanilino)phthalimide Monoclinic	Triclinic
C1—O1	1.224 (6)	1.229 (3)	1.208 (3)	1.204 (2)	1.202 (2)
C8—O2	1.215 (5)	1.209 (3)	1.203 (3)	1.205 (2)	1.206 (2)
C1—N1	1.406 (6)	1.385 (3)	1.397 (4)	1.405 (2)	1.409 (2)
C8—N1	1.415 (6)	1.412 (3)	1.406 (4)	1.398 (2)	1.392 (2)
C1—C2	1.475 (7)	1.468 (4)	1.482 (4)	1.479 (2)	1.474 (3)
C2—C3	1.379 (7)	1.375 (4)	1.374 (4)	1.375 (2)	1.376 (3)
C2—C7	1.407 (6)	1.404 (3)	1.381 (4)	1.394 (2)	1.387 (3)
C3—C4	1.398 (8)	1.387 (4)	1.383 (5)	1.387 (3)	1.379 (3)
C4—C5	1.386 (8)	1.393 (5)	1.385 (5)	1.380 (3)	1.384 (3)
C5—C6	1.388 (6)	1.366 (4)	1.368 (5)	1.383 (2)	1.377 (3)
C6—C7	1.376 (7)	1.375 (4)	1.379 (4)	1.374 (2)	1.378 (3)
C7—C8	1.479 (6)	1.478 (4)	1.489 (4)	1.482 (2)	1.480 (3)
C9—C14	1.397 (6)	1.374 (4)	1.382 (4)	1.380 (2)	1.390 (3)
C9—C10	1.403 (7)	1.392 (4)	1.378 (5)	1.377 (2)	1.398 (2)
C9—N2	1.402 (6)	1.413 (4)	1.427 (4)	1.425 (2)	1.401 (2)
C10—C11	1.379 (7)	1.382 (5)	1.383 (5)	1.388 (3)	1.371 (3)
C11—C12	1.368 (8)	1.369 (6)	1.370 (6)	1.363 (3)	1.377 (3)
C12—C13	1.397 (7)	1.374 (5)	1.368 (6)	1.373 (3)	1.373 (3)
C13—C14	1.371 (7)	1.386 (5)	1.385 (5)	1.386 (3)	1.378 (3)
N1—N2	1.396 (5)	1.381 (3)	1.392 (4)	1.396 (2)	1.383 (2)
C15—N2	—	—	—	1.460 (2)	1.459 (3)

Table 7. *Values of selected bond, torsion and interplanar angles (°) for the four polymorphs of N-anilinophthalimide and N-(N′-methylanilino)phthalimide; the values have been calculated from the coordinates given in Tables 2–5; the signs of the torsion angles have only relative significance*

Angle	*N*-Anilinophthalimide α (orthorhombic) polymorph	*N*-Anilinophthalimide β (monoclinic) polymorph Molecule *A*	*N*-Anilinophthalimide β (monoclinic) polymorph Molecule *B*	*N*-(*N*′-Methylanilino)phthalimide α (monoclinic) polymorph	*N*-(*N*′-Methylanilino)phthalimide β (triclinic) polymorph
N1—N2—C9	115.9 (4)	118.3 (2)	117.3 (3)	114.30 (13)	116.42 (14)
C1—N1—N2—C9	69.1 (6)	88.2 (3)	87.8 (4)	−72.6 (2)	70.2 (2)
N1—N2—C9—C14	32.1 (6)	15.0 (4)	9.1 (5)	−45.0 (2)	10.8 (2)
O1—C1—N1—N2	−0.4 (7)	−0.6 (4)	−4.7 (4)	0.4 (3)	−0.8 (3)
C1—N1—N2—C15	—	—	—	67.3 (2)	78.8 (2)
Between planes N1, C1 to C8 and C9 to C14	91.8	89.1	88.6	85.06 (5)	73.7
Σ(angles about N1)	360.0 (7)	358.6 (3)	359.6 (5)	360.0 (2)	360.0 (2)
Σ(angles about N2)	342 (4)	346 (3)	339 (3)	346.0 (2)	351.8 (3)

Table 8. *Hydrogen-bonding geometry (Å, °) in the two polymorphs of N-anilinophthalimide*

N2—H···O=C	*d*(N—H)	*d*(N···O)	*d*(H···O)	N—H···O	(N—)H···O=C
Orthorhombic phase					
$N2^{i}$—H···$O2^{ii}$	0.87 (5)	3.407 (6)	2.56 (5)	167 (3)	120 (3)
Monoclinic phase (O2*A* and O2*B* do not participate in hydrogen bonding)					
$N2A^{iii}$—H2N*A*···$O1A^{ii}$	0.86 (3)	3.095 (3)	2.25 (3)	170 (2)	132 (2)
$N2B^{iii}$—H2N*B*···$O1A^{ii}$	0.93 (4)	3.191 (3)	2.31 (3)	158 (2)	112 (2)
$N2A^{ii}$—H2N*A*···$O1B^{ii}$	0.86 (4)	3.144 (3)	2.78 (3)	108 (2)	153 (2)

Possible carbonyl···nitrogen interaction: $d(O1B^{ii}\cdots N1A^{ii})$ = 2.969 (4) Å; $N2A^{i}$—$N1A^{i}$—$O1B^{i}$ = 84.1 (4), $C1B^{i}$—$O1B^{i}\cdots N1A^{i}$ = 153.4 (4)°. Symmetry codes: (i) *x*, *y*, 1 − *z*; (ii) *x*, *y*, *z*; (iii) 1 − *x*, −*y*, −*z*.

[*d*(C=)O1*B*···N1*A* = 2.969 (4) Å]; the carbonyl is approximately perpendicular to the phthalimide plane. Perhaps the most surprising result from the crystal structure analyses of *N*-anilinophthalimide is that there is only very weak hydrogen bonding between molecules in the orthorhombic polymorph and weak hydrogen bonding in the monoclinic polymorph.

5.2. *Formalities of the phase transformation in N-anilinophthalimide*

The space group of the orthorhombic phase is $P2_12_12_1$, which is chiral. Thus, spontaneous resolution of enantiomers has taken place on crystallization. If the torsion angles about N1—N2 and N2—C9 were 90 and

0°, respectively, then the molecule would have C_s–m symmetry, with the mirror plane containing the phenyl ring bisecting the phthalimide portion. As the torsion angle about N1—N2 is 69° and that about N2—C9 is 32° (Table 7), two enantiomeric pairs of diastereoisomeric rotamers are possible, in principle, corresponding to the four sign combinations of the torsion angles about N1—N2 and N2—C9. In practice, in a particular crystal, only one of the pairs is found, that corresponding to the combination +69/+32°; as the absolute configuration of the crystal used in the structure analysis was not determined, these signs have relative and not absolute significance. Of course, racemization will be immediate on solution.

The monoclinic phase is racemic so that the corresponding torsion angles are +88/+15°and +88/+9° for one *A*, *B* pair of crystallographically independent molecules and their negative counterparts for the other pair (again the signs have relative and not absolute significance). Racemization must occur during the solid-state transformation; this will involve a minor change from a +69/+32° to a +88/+15° (say) conformation and a somewhat larger change from +69/+32° to −88/−9° (say). The molecular arrangements in the two phases (Figs. 2 and 3) are quite different, but only van der Waals interactions are involved and no immediate explanation for the hysteresis appears from the crystal structures.

5.3. *Thermal expansion of N-anilinophthalimide*

Single crystals of both phases were sealed into capillaries and mounted on a Nonius crystal heating device (Tuinstra & Fraase Storm, 1978) modified for attachment to the Philips PW 1100/20 four-circle diffractometer. The temperature scale was calibrated by reference to the melting points of a number of standard compounds. Cell dimensions were measured using Mo $K\alpha$. The temperature range for the monoclinic phase was 293–384 K and a little less for the orthorhombic phase; splitting of reflections at the high-temperature ends of these ranges showed that the crystals were beginning to incur damage of an unspecified kind. The cell dimensions and volumes increased monotonously with temperature for both phases; values are deposited.† The volume–temperature relations are shown in Fig. 4; ΔV(ortho→mono) is 5.73 Å^3 per molecule at 293 K and 5.63 at 370 K.

5.4. *Analysis of thermal vibrations of N-anilinophthalimide and of N-(N′-methylanilino)phthalimide*

The thermal motion in the two phases of *N*-anilinophthalimide has been analyzed with the program *THMA* (version of 15 April, 1987); for a summary of recent developments in this area, see Dunitz, Maverick & Trueblood (1988) and Dunitz, Schomaker & Trueblood (1988). Firstly, each of the three independent molecules was treated as an entire rigid body and then libration of the phenyl group was introduced, both about the N1—N2 and N2—C9 bonds. The *R* values obtained for observed and calculated values of U^{ij} for all non-H atoms are summarized in Table 9. It is clear that the best results are obtained if allowance is made for libration about N1—N2 and only these results are reported. The eigenvalues are given in the inertial frame (Table 10). In general, the degree of thermal motion is much the same for all three molecules, although an overall assessment suggests, as expected, that ADP's are a little less in the orthorhombic than in the monoclinic phase. The translational motion is roughly isotropic and thus the directions of the translational principal axes with respect to the molecular axes are not well determined. Although the librational motions are rather anisotropic, there are no clear angular relationships to the molecular axes of inertia. The librational amplitudes of the phenyl groups are very similar in the three molecules. Correction of bond lengths for librational motions adds 0.003–0.011 Å to bond lengths, depending on their location in the molecules.

The thermal motion in the two phases of *N*-(*N*′-methylanilino)phthalimide has been analyzed with *THMA* (version of 7 June, 1991). The same pattern of analysis was used as for *N*-anilinophthalimide and it is again clear that the best results are obtained if the effects of libration about N1—N2 are included, and only these results are reported. The librational amplitudes in the triclinic phase are slightly larger than those in the monoclinic phase, but the differences are not

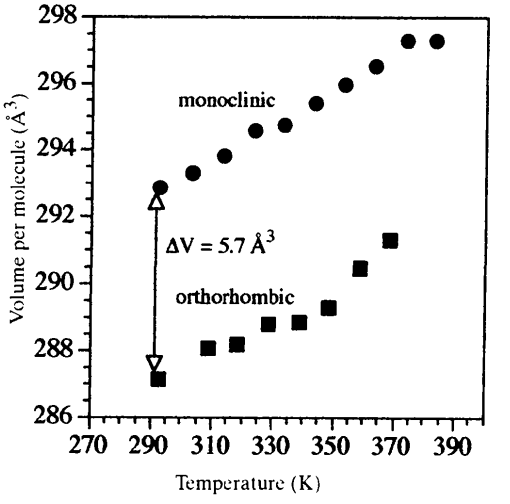

Fig. 4. Graphs of volume (Å^3) per molecule in the orthorhombic and monoclinic phases of *N*-anilinophthalimide as a function of temperature.

† See deposition footnote on p. 279.

Table 9. *Weighted R values for thermal motion analysis without and with allowance for effects of libration of phenyl groups for the polymorphs of N-anilinophthalimide and N-(N′-methylanilino)phthalimide*

U^{ij}'s are given in the crystal systems $\Delta(U^{ij}) = U^{ij}(\text{obs}) - U^{ij}(\text{calc})$; $R(U^{ij}) = [\{\Sigma[\Delta(U^{ij})]^2\}/\{\Sigma[U^{ij}(\text{obs})^2]\}]^{1/2}$; the bracketed values are for the diagonal values U^{ii} only.

Molecule	Rigid body	Libration about N2—C9	Libration about N1—N2
N-Anilinophthalimide			
Orthorhombic	0.155 (0.112)	0.144 (0.106)	0.134 (0.098)
Monoclinic *A*	0.155 (0.118)	0.154 (0.116)	0.108 (0.092)
Monoclinic *B*	0.162 (0.124)	0.155 (0.119)	0.110 (0.100)
N-(*N*′-Methylanilino)phthalimide			
Monoclinic	0.142 (0.112)	0.122 (0.093)	0.115 (0.086)†
Triclinic	0.144 (0.099)	0.135 (0.096)	0.106 (0.076)

† Model or data suspect.

Table 10. *Translation and libration amplitudes (Å, °) of the molecules in the polymorphs of N-anilinophthalimide and N-(N′-methylanilino)phthalimide; the libration amplitude Φ (°) of the phenyl group about the N1—N2 bond is given for both molecules in all the polymorphs*

Molecule	*T*1	*T*2	*T*3	*L*1	*L*2	*L*3	Φ
N-Anilinophthalimide							
Orthorhombic	0.265	0.209	0.195	5.08	2.94	1.19	5.01
Monoclinic *A*	0.229	0.224	0.214	4.90	3.19	2.24	4.80
Monoclinic *B*	0.262	0.244	0.208	5.00	3.81	2.54	4.98
N-(*N*′-Methylanilino)phthalimide							
Monoclinic	0.225	0.213	0.202	5.63	2.82	1.94	5.60
Triclinic	0.238	0.211	0.208	6.33	2.86	2.21	6.26

striking. There is also a similar lack of striking differences when the thermal motion is compared in the two phases of pyridinium picrate (Botoshansky *et al.*, 1994*b*).

5.5. *Molecular packing in the polymorphs of N-(N′-methylanilino)phthalimide*

The packing arrangements in the two polymorphs are illustrated in the stereo diagrams of Figs. 5 and 6. Hydrogen bonding is not possible and there are no carbonyl···nitrogen interactions; we have not been able to detect any resemblances between the two packing arrangements. In the monoclinic polymorph centrosymmetrically related pairs of molecules are in columns along the ~11 Å *c* axis; the phthalimide planes are antiparallel and the phenyls protrude outside the columns. The columns along the central axes of the cells are related to those at the corners by the *c*-glide and the long axes of the molecules are approximately mutually perpendicular. In the triclinic polymorph there are columns of translationally related molecules along the ~5.7 Å *a* axis and sheets of columns in (001) planes. Alternate sheets have the long axes of the molecules pointing in opposite directions. Presumably there should be good cleavage along (001), but this has not been checked.

5.6. *Formalities of the phase transformation in N-(N′-methylanilino)phthalimide*

As both polymorphs are centrosymmetric, racemization is not an issue. The occurrence of a broad endotherm (Fig. 10 below) suggests that a phase intermediate between monoclinic and triclinic may form, but we have not attempted an investigation. The main conformational change in the overall transformation 'monoclinic to triclinic' is in the relative dispositions of phenyl and phthalimide rings, *i.e.* in the torsion angle N1—N2—C9—C14 and the interplanar angle between phthalimide and phenyl planes (Table 7).

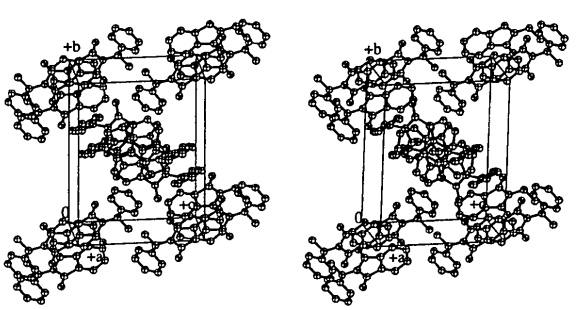

Fig. 5. *ORTEP*II (Johnson, 1976) stereodiagram showing the packing in the monoclinic polymorph of *N*-(*N*′-methylanilino)phthalimide; viewed approximately down [001]. Details as for Fig. 1.

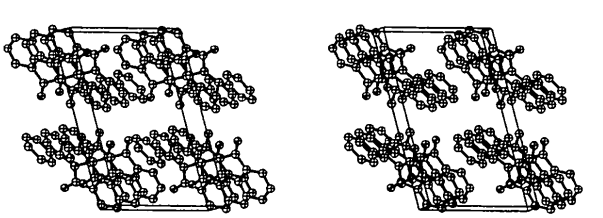

Fig. 6. *ORTEP*II (Johnson, 1976) stereodiagram showing the packing in the triclinic polymorph of *N*-(*N*′-methylanilino)phthalimide; viewed approximately down [100]. Details as for Fig. 1.

6. Thermal and solubility behavior of the polymorphs of *N*-anilinophthalimide

6.1. *Deductions from solubility measurements*

CL15 measured the solubilities of both polymorphs in a number of solvents and determined the temperature at which the polymorphs are in thermodynamic equilibrium. Elementary theory (Swalin, 1972) gives $\ln X = \ln A - \Delta H_{soln}/RT$, where X is the mole fraction of solute in the saturated solution at temperature T and ΔH_{soln} is the enthalpy of solution, assumed to be constant over the temperature range of the measurements. Thus, the slope of a plot of $\ln X$ against $1/T$ will give $\Delta H_{soln}/R$, which will depend both on the polymorph considered and the solvent. We have calculated such plots for all the data given by CL15 and the results are included in Table 11; the plots are not reproduced.

If there are two polymorphs A and B, then we can write $\ln(X_A/X_B) = \ln(A_A/A_B) - [(\Delta H_A - \Delta H_B)/RT]$, where ΔH_i are the enthalpies of solution of the polymorphs. Thus, the slope of a plot of $\ln (X_A/X_B)$ against $1/T$ will give $[(\Delta H_A - \Delta H_B)/R]$, where $(\Delta H_A - \Delta H_B) = \Delta H_{transf}$ is the enthalpy of transformation of A into B, which depends only on the polymorphs and not on the solvent. The differences in solubility of the two polymorphs in a particular solvent are small and are not clearly shown, even on large-scale plots such as those in Figs. 1 and 2 of CL15. Furthermore, the accuracy of these measurements was not reported and there does not seem to be any way of making an assessment (see *Appendix*). Nevertheless, the values reported are internally consistent and we shall proceed on the assumption that they are reliable. We show in Fig. 7 the solubility ratio as a function of temperature, where the solubilities are expressed as the number of grams of solute in 100 g of saturated solution, and are taken directly from CL15; the small deviations of these values from unity should be noted. We deduce a transformation temperature for *N*-anilinophthalimide of 283 K, compared with the CL15 value of 282.4 K.

The solubilities have been converted into mole fractions of solute in the saturated solution and the $\ln(X_1/X_2)$ values are plotted against $1/T$ in Fig. 8; the direction of the reciprocal temperature axis has been reversed for ease of comparison with the previous figure. Although there seems to be a definite concavity of the data with respect to the abscissa, we have ignored this in calculating a mean slope on a linear approximation, obtaining $\Delta H_{transf} = 1.54$ kJ mol^{-1}. Analogous values can also be calculated from the pairwise differences between the enthalpies of solution of the two polymorphs in the various solvents (Table 11); there is good agreement.

6.2. *Solubility behavior of the polymorphs of N-(N'-methylanilino)anilinophthalimide*

Detailed solubility–temperature measurements for the *N*-(*N'*-methylanilino)phthalimide polymorphs were made by CL15 apparently only for ethanol; we calculate from these measurements that the enthalpy of solution

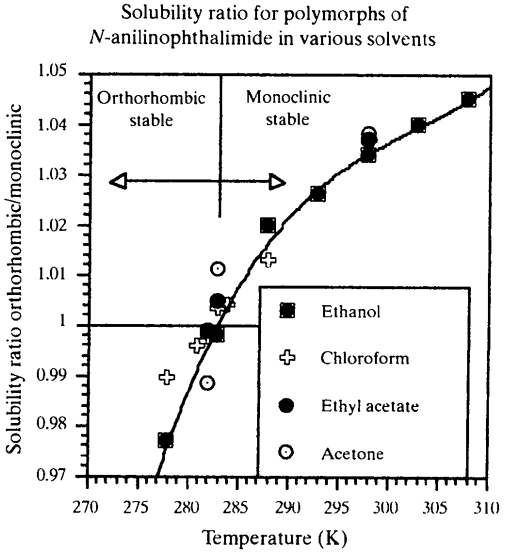

Fig. 7. The ratio of the solubilities of the orthorhombic and monoclinic polymorphs as a function of temperature; measurements from CL15. The various solvents are designated and the data points clearly represent a single set. The curve is a guide to the eye.

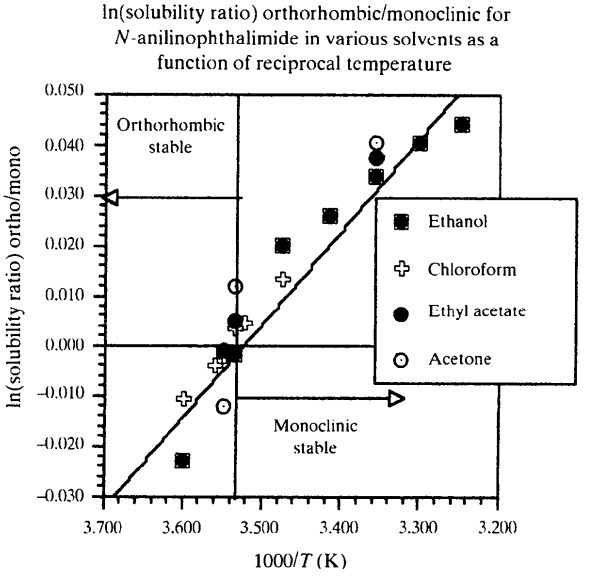

Fig. 8. The natural logarithm of the ratio of the mole fractions in saturated solutions of the two polymorphs of *N*-anilinophthalimide (orthorhombic/monoclinic) plotted against the reciprocal absolute temperature; measurements from CL15. The direction of the abscissa has been reversed so as to have the lower temperatures at the left.

Table 11. *Some details of the solubility data for the two polymorphs of N-anilinophthalimide in various solvents, as given by CL15, or as calculated from their results*

The solubilities are given at 298 K as grams of solute in 100 g saturated solution. X_{solute} is the mole fraction of solute in the saturated solution, ΔH_{soln} is the enthalpy of solution in units of kJ mol^{-1} calculated from plots of ln X_{solute} against $1/T$ and ΔH_{transf} is the enthalpy of transformation from orthorhombic to monoclinic polymorphs (in kJ mol^{-1}), as calculated from the differences in the enthalpies of solution of the two polymorphs for the various solvents.

	Orthorhombic polymorph			Monoclinic polymorph			
Solvent and temperatures (K) of measurement	Solubility	X_{solute}	ΔH_{soln}	Solubility	X_{solute}	ΔH_{soln}	ΔH_{transf}
Ethanol (278, 283, 288, 293, 298, 303, 308)	0.913	0.00178	26.94	0.883	0.00172	25.40	1.54
Chloroform (278, 281, 282, 283, 284, 288, 298)	4.484	0.0230	15.88	4.324	0.0222	14.21	1.67
Ethyl acetate (282, 283, 298)	4.654	0.0178	27.2	4.489	0.0171	25.6	1.6
Acetone (282, 283, 298)	10.060	0.0265	12.9	9.693	0.0255	11.0	1.9

Table 12. *Some details of the solubility data for the two polymorphs of N-(N′-methylanilino)phthalimide in ethanol, as given by CL15, or as calculated from their results*

The solubility is given at 298 K as grams of solute in 100 g saturated solution. ΔH_{soln} is the enthalpy of solution in units of kJ mol^{-1}, X_{solute} is the mole fraction of solute in the saturated solution and ΔH_{transf} is the enthalpy of transformation from the monoclinic to triclinic polymorph (in kJ mol^{-1}), as calculated from the differences in the enthalpies of solution of the two polymorphs for ethanol. The solubility of *N*-(*N*′-methylanilino)phthalimide in methanol at 303 K is given as 4.547 and 5.033 g/100 g saturated solution for the monoclinic and triclinic polymorphs, respectively.

	Monoclinic polymorph			Triclinic polymorph			
Solvent and temperatures (K) of measurement	Solubility	X_{solute}	ΔH_{soln}	Solubility	X_{solute}	ΔH_{soln}	ΔH_{transf}
Ethanol (278, 283, 288, 293, 298, 303, 308)	1.697	0.003143	34.95	1.931	0.003583	30.78	4.17

of the monoclinic polymorph is 34.95 kJ mol^{-1} and that of the triclinic polymorph is 30.78 kJ mol^{-1}; thus, ΔH_{transf} = 4.17 kJ mol^{-1} (Table 12).

6.3. *DSC measurements for N-anilinophthalimide*

DSC scans (Polymer Laboratories DSC System) were made for the orthorhombic and monoclinic polymorphs of *N*-anilinophthalimide (~10 mg samples) over the temperature range 253–473 K. The orthorhombic polymorph showed endotherms on heating at ~401 K (ΔH_{transf} = 1.62 kJ mol^{-1}) and 457 K (ΔH_{fus} = 26.9 kJ mol^{-1}; Fig. 9). The first endotherm corresponds to the transition orthorhombic to monoclinic and the second to melting of the monoclinic phase. The (heating–cooling) trace for the monoclinic polymorph showed only the melting endotherm and the solidification exotherm. There was no sign of any thermal event (for either polymorph) in the vicinity of 283 K, the thermodynamic transition temperature. Our results agree with those of CW11, where it is stated 'if large crystals of the pale yellow form are heated to 100°C, deep yellow spots quickly appear...after some hours heating, the latter are transformed into opaque paramorphs of the yellow modification. This transformation is much more rapid at a higher temperature...'.

6.4. *DSC measurements for N-(N′-methylanilino)-phthalimide*

DSC scans (Polymer Laboratories DSC System) were made for the monoclinic and triclinic polymorphs (~2.5 mg samples) over the temperature range 290–410 K. The monoclinic polymorph showed a broad endotherm on heating at ~372–376 K (total ΔH_{transf} = 3.60 kJ mol^{-1}) and 399 K (ΔH_{fus} = 21.7 kJ mol^{-1}), Fig. 10. The broad endotherm corresponds to the overall transition monoclinic to triclinic and the second to melting of the triclinic phase; we have not attempted to investigate the broad endotherm in detail. The (heating–cooling) trace for the triclinic polymorph showed only the melting endotherm and the solidifica-

tion exotherm. There was no sign of any thermal event (for either polymorph) in the vicinity of 328 K, the thermodynamic transition temperature. The DSC measurements were made at scan speeds of 2 and 5° min^{-1}; the same temperatures were obtained for the broad endotherms, but the value of ΔH_{transf} was approximately twice as large at the slower scan speed; ΔH_{fus} was much less sensititve. Our results agree with those of CW11, where it is stated 'crystals of the pale yellow modification of phthalylphenylmethylhydrazide...transform quickly into the orange when heated to the neighbourhood of 100°C, while the orange-coloured crystals when dry remain unchanged for months at the ordinary temperature'. The (metastable) melting point of the monoclinic phase (387 K) was determined using a microscope hot stage and was not detected in the DSC traces.

7. Discussion

7.1. *Polymorphism of N-anilinophthalimide*

We compare our results with some features of polymorphism pointed out by GF95. Firstly, the *N*-anilinophthalimide cluster has a (unit cell) volume change at the transition $\Delta V_{transf} = V_{monoclinic} - V_{orthorhombic} = +1.88\%$; ~95% of the clusters cited by GF95 show a volume expansion on passing through the transition. Secondly, the *N*-anilinophthalimide cluster has one molecule in the asymmetric unit of the orthorhombic

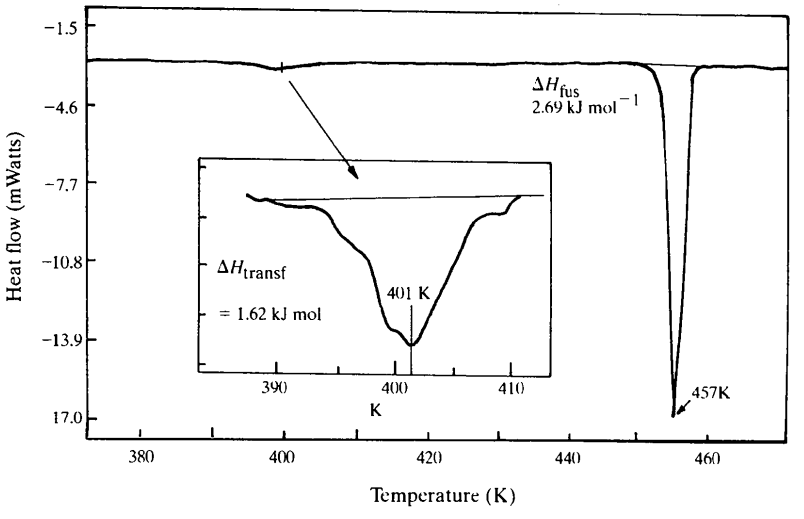

Fig. 9. DSC trace for the orthorhombic polymorph of *N*-anilinophthalimide. Fusion and solid-state transformation endotherms are shown; note that the former is much sharper than the latter. An analogous trace for the monoclinic polymorph is featureless apart from the melting endotherm.

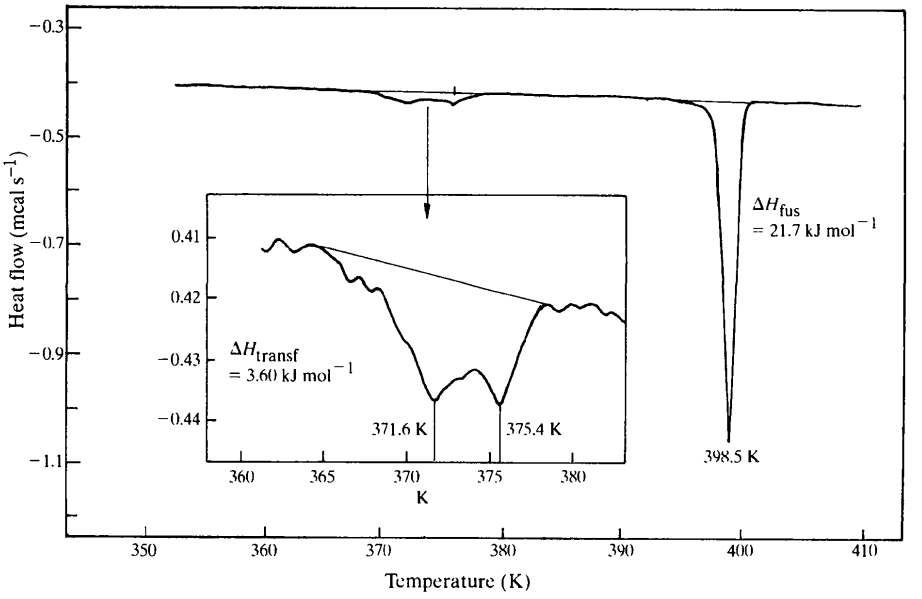

Fig. 10. DSC trace for the monoclinic polymorph of *N*-(*N'*-methylanilino)phthalimide. Fusion and solid-state transformation endotherms are shown; note that the form of the latter suggests the occurrence of two phase transformations. An analogous trace for the triclinic polymorph is featureless apart from the melting endotherm.

polymorph and two in that of the monoclinic polymorph; 28% of the clusters in the GF95 sample show this feature (see their Fig. 1*d*). Thirdly, this cluster has a $P2_12_12_1$–$P2_1/a$ combination; 24% of the couples in the GF95 sample 'comprise a centrosymmetric and non-centrosymmetric partner', 5% of the total (10 couples) having the $P2_12_12_1$–$P2_1/a$ combination. Finally, the entropy of transition is calculated from $\Delta G_{transf} = \Delta H_{transf} - T_c\Delta S_{transf} = 0$ at the transition temperature T_c: ΔS_{transf} = (4.2 kJ mol^{-1})/283 K = 14.8 J mol^{-1} K^{-1}; GF95 comment that 'differences [in vibrational entropy of two polymorphs] never exceed 15 J mol^{-1} K^{-1}'. Our value of ΔH_{transf} (1.6 kJ mol^{-1}; see below) fits in at the lower end of the set of values given by GF95 in their Table 1. The entropy of fusion is calculated from ΔS_{fus} = (26.9 kJ mol^{-1}/457.2 K) = 58.8 J mol^{-1} K^{-1}.

7.2. *Polymorphism of N-(N′-methylanilino)phthalimide*

We next consider the transition in *N*-(*N*′-methylanilino)phthalimide. Firstly, the cluster has a (unit cell) volume change at the transition $\Delta V = V_{triclinic} - V_{monoclinic}$ = 0.7%. Secondly, both polymorphs have one molecule in the asymmetric unit; 72% of the clusters in the GF95 sample show this feature. Thirdly, the cluster has a $P2_1/c$–$P\bar{1}$ combination; it is not known how many of the couples in the GF95 sample had this combination. Finally, the entropy of transition at the transition temperature T_c is ΔS_{transf} = (4.17 kJ mol^{-1})/328.4 K = 12.7 J mol^{-1}K^{-1}; the entropy of fusion is calculated from ΔS_{fus} = (21.71 kJ mol^{-1}/398.7 K) = 54.45 J mol^{-1} K^{-1}.

8. Conclusions

There is a common pattern of phase behavior to the systems Tl^{I} picrate, pyridinium picrate, *N*-anilinophthalimide and *N*-(*N*′-methylanilino)phthalimide. These systems are characterized by having first-order enantiotropic phase transitions, with considerable hysteresis so that there is an appreciable difference between thermodynamic (equilibrium) and DSC-measured (kinetic) transition temperatures; ΔH_{transf} is a few per cent of ΔH_{fus} (both endothermic) and ΔV is positive and a few per cent of the cell volumes. Another compound studied in rather similar fashion to the systems discussed here is sulfamerazine [4-amino-*N*-(4-methyl-2-pyrimidinyl)benzenesulfonamide (Caira & Mohamed, 1992)], which has two orthorhombic phases containing similar hydrogen-bonded dimers, but with different intermolecular hydrogen-bonding schemes; the formal similarity in behavior is strikingly illustrated by comparing Fig. 2 of Caira & Mohamed (1992) with our Figs. 9 and 10. We venture to suggest that 422 K is not the equilibrium T_c for sulfamerazine. Dimethyl 3,6-dichloro-2,5-dihydroxyterephthalate, discussed by Katrusiak (1996), also resembles the present systems in its phase behavior, the two polymorphs having different hydrogen-bond arrangements. When there are differences in hydrogen bonding between the phases (as in sulfamerazine, dimethyl 3,6-dichloro-2,5-dihydroxyterephthalate and, in a somewhat different sense, pyridinium picrate) it is possible to provide a description of the differences in the structural arrangements, which will, hopefully, be translated into energy differences. This is much more difficult when, as in the present study, there are only van der Waals interactions (or even rather weak hydrogen bonding) between the molecules. Indeed, the crystal structures of neither cluster of polymorphs give hints explaining the occurrence of the phase transformations in the system, nor is it clear why there should be hysteresis. Insofar as hysteresis is concerned, it seems necessary to invoke crystal imperfections of some kind, presumably in the sense of the inhibition of the formation of suitable nucleation sites for growth of the high-temperature phase on heating. The absence of a reverse transformation on cooling is perhaps due to the slowing down of diffusion below the transition temperatures. The need for suitable nucleation sites has previously been stressed by Kitaigorodskii *et al.* (1965) and Mnyukh (1976) in their studies of the enantiotropic monoclinic to triclinic phase transformation in *p*-dichlorobenzene.

APPENDIX *A*

As we have noted above, there does not seem to be any way of assessing the accuracy of the solubility measurements, apart, perhaps, from their internal

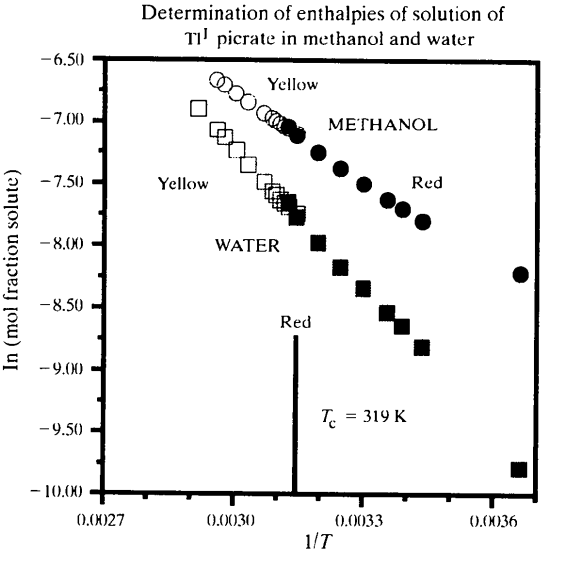

Fig. 11. The solubilities of the red and yellow phases of thallium(I) picrate in methanol and water as a function of temperature, recalculated from the original values of Rabe (1901).

Table 13. *Enthalpies of solution and transition in units of kJ mol^{-1} for the two polymorphs of Tl^{I} picrate in methanol and water, as calculated from the solubility measurements of Rabe (1901), see also Fig. 11*

ΔH_{soln} is the enthalpy of solution and ΔH_{transf} is the enthalpy of transformation from the red to yellow polymorph, as calculated from the differences in the enthalpies of solution of the two polymorphs for methanol and water.

Solvent	ΔH_{soln} for red polymorph	ΔH_{soln} for yellow polymorph	ΔH_{transf}
Methanol	18.14	19.52	−1.38
Water	31.85	31.41	0.44
DSC	-	-	5.0

consistency. As an illustration of possible pitfalls we consider the solubility measurements of Rabe (1901) for the Tl^{I} picrate polymorphs, shown in Fig. 10 of Botoshansky *et al.* (1994*a*) and redrawn here on a logarithmic scale (Fig. 11). The enthalpies of solution of the polymorphs in methanol and water are given in Table 13; the enthalpy of transition determined from the methanol solubilities is exothermic and hence qualitatively wrong; for water the quantitative agreement between the value determined from the solubilities (0.44 kJ mol^{-1}) and that measured by DSC (5.0 kJ mol^{-1}; Botoshansky *et al.*, 1994*b*) is poor.

We are grateful to Professor A. Siegmann (Materials Engineering, Technion) for access to the Mettler Differential Scanning Calorimeter and to the Vice President for Research and the Fund for the Promotion of Research at Technion for financial support. We acknowledge with thanks support for Dr Botoshansky from the Israel Ministry for Science and Technology. We thank (the late) Professor Dan Becker, Dr Amnon Stanger and Dr Vitaly Steiman (all Technion) for their assistance with the chemistry. A special word of thanks is due to Dr C. K. Prout (Chemical Crystallography Laboratory, University of Oxford) for attempting (unfortunately without success) to locate the materials prepared and studied by Chattaway and Barker.

References

Barlow, J. H., Davidson, R. S., Lewis, A. & Russell, D. N. (1979). *J. Chem. Soc. Perkin Trans. 2*, pp. 1103–1109.
Becker, D., Botoshansky, M., Gasper, N., Herbstein, F. H. & Karni, M. (1998). *Acta Cryst.* B**54**. In the press.
Botoshansky, M., Herbstein, F. H. & Kapon, M. (1994*a*). *Acta Cryst.* B**50**, 191–200.
Botoshansky, M., Herbstein, F. H. & Kapon, M. (1994*b*). *Acta Cryst.* B**50**, 589–596.
Caira, M. R. & Mohamed, R. (1992). *Acta Cryst.* B**48**, 492–498.
Chattaway, F. D. & Lambert, W. J. (1915). *J. Chem. Soc.* **107**, 1773–1781.
Chattaway, F. D. & Wünsch, D. F. S. (1911). *J. Chem. Soc.* **99**, 2253–2265.
Cohen, E. (1929). *J. Soc. Chem. Ind.* **48**, 162–168.
Cohen, E. & Moesveld, A. L. Th. (1920). *Z. Phys. Chem.* **38**, 450–464.
Dunitz, J. D. & Bernstein, J. (1995). *Accts. Chem. Res.* **28**, 193–200.
Dunitz, J. D., Maverick, E. F. & Trueblood, K. N. (1988). *Angew. Chem. Intl. Ed. Engl.* **27**, 880–895.
Dunitz, J. D., Schomaker, V. & Trueblood, K. N. (1988). *J. Phys. Chem.* **92**, 856–867.
Dunlap, F. L. (1905). *J. Am. Chem. Soc.* **27**, 1091–1107.
Gavezzotti, A. & Filippini, G. (1995). *J. Am. Chem. Soc.* **117**, 12299–12305.
Herbstein, F. H. (1996). *J. Mol. Struct.* **374**, 111–128.
Herbstein, F. H., Kapon, M. & Wielinski, S. (1977). *Acta Cryst.* B**33**, 649–654.
Johnson, C. K. (1976). *ORTEP*II. Report ORNL-5138. Oak Ridge National Laboratory, Oak Ridge, Tennessee.
Katrusiak, A. (1996). *Cryst. Rev.* **5**, 133–180.
Kitaigorodskii, A. I., Mnyukh, Yu. V. & Asadov, Yu. V. (1965). *J. Phys. Chem. Solids*, **26**, 463–472.
Macicek, J. & Yordanov, A. (1992). *J. Appl. Cryst.* **25**, 73–80.
Mnyukh, Yu. V. (1976). *J. Cryst. Growth*, **32**, 371–377.
Philips (1973). *PW*1100/20 *Software*. Natuurkundig Laboratorium, NV Philips Gloeilampenfabrieken, Eindhoven, The Netherlands.
Rabe, W. O. (1901). *Z. Phys. Chem.* **38**, 175–184.
Rao, C. N. R. & Gopalakrishnan, J. (1989). *New Directions in Solid State Chemistry*, Table 4.1, p. 149. Cambridge University Press.
Sheldrick, G. M. (1990). *Acta Cryst.* A**46**, 467–473.
Sheldrick, G. M. (1993). *SHELXL*93. *Program for the Refinement of Crystal Structures*. University of Göttingen, Göttingen, Germany.
Siemens (1989*a*). *P3/PC Diffractometer Program*. Version 3.13. Siemens Analytical X-ray Instruments Inc., Madison, Wisconsin, USA.
Siemens (1989*b*). *XDISK. Data Reduction Program*. Version 3.11. Siemens Analytical X-ray Instruments Inc., Madison, Wisconsin, USA.
Swalin, R. A. (1972). *Thermodynamics of Solids*, 2nd ed. New York: Wiley Interscience.
Taylor, R. & Kennard, O. (1986). *Acta Cryst.* B**42**, 112–120.
Tuinstra, F. & Fraase Storm, G. M. (1978). *J. Appl. Cryst.* **11**, 257–259.